On the influence of a surface roughness on propagation of anti-plane short-length localized waves in a medium with surface coating

Gennadi I. Mikhasev [a,*], Marina G. Botogova [a], Victor A. Eremeyev [b,c,d]

[a] *Belarusian State University, Minsk, Belarus*
[b] *Department of Civil and Environmental Engineering and Architecture (DICAAR), University of Cagliari, Via Marengo, 2, Cagliari 09123, Italy*
[c] *Faculty of Civil and Environmental Engineering, Gdańsk University of Technology, ul. Gabriela Narutowicza 11/12 Gdańsk 80-233, Poland*
[d] *R. E. Alekseev Nizhny Novgorod Technical University, Minin St., 24, Nizhny Novgorod 603950, Russia*

A B S T R A C T

We discuss the propagation of localized surface waves in the framework of the linear Gurtin–Murdoch surface elasticity and taking into account a roughness of a free boundary. We derive a boundary-value problem for anti-plane motions with curvilinear boundary and surface stresses. Using the asymptotic technique developed earlier, we obtain the form of a localized wave and analyze its amplitude evolution. As the main result we present the dependence of the wave amplitude on the roughness magnitude. The presented results could be used for non-destructive evaluation of the surface microstructure using surface waves-based devices. In particular, measuring the decay rate with the depth one can estimate roughness of a surface and appearance of new surface defects.

1. Introduction

Actual advances in engineering of micro- and nano-electromechanical systems (MEMS and NEMS) such as sensors and actuators result in a certain extension of the classic continuum and structural mechanics towards application of new non-classic models. In particular, nowadays it is rather well established that material properties at small scales may be essentially different from their counterparts at the macroscale. In other words, we can observe so-called size-effect which could be explained on the base of some generalized models of continua. Among these models it is worth to mention the surface elasticity approach which extends the notion of surface tension in fluids to more complex phenomena in solids. The most used models of the surface elasticity were proposed by Gurtin and Murdoch (1975, 1978) and by Steigmann and Ogden (1997, 1999). These models found various applications in the mechanics at the nanoscale, see, *e.g.*, Duan, Wang, and Karihaloo (2008), Wang et al. (2011), Kim, Ru, and Schiavone (2013), Eremeyev (2016), Han, Mogilevskaya, and Schillinger (2018), Gorbushin, Eremeyev, and Mishuris (2020), Zemlyanova (2020) and Doan, Le-Quang, and To (2020), where various problems of mechanics of nanostructured materials are considered. From the physical point of view the surface elasticity approach describes finite or infinitesimal deformations of a solid body with attached on its surface an

* Corresponding author.
E-mail addresses: Mikhasev@bsu.by (G.I. Mikhasev), Batahova@bsu.by (M.G. Botogova), eremeyev.victor@gmail.com (V.A. Eremeyev).

elastic membrane or a shell. For discussion of the surface stresses nature we also refer to Murdoch (2005), Huang and Wang (2006), Duan et al. (2008) and Ru (2010). In particular, the boundary conditions on a surface or interface within the linear surface elasticity are similar to ones found for coatings of finite thickness and for so-called rigidly stiff interfaces analyzed by Benveniste (2006), Benveniste and Miloh (2001), Benveniste and Berdichevsky (2010), Mishuris, Movchan, and Movchan (2006), Mishuris, Movchan, and Movchan (2010), Kaplunov and Prikazchikov (2017) and Baranova, Mogilevskaya, Nguyen, and Schillinger (2020), see also recent discussions by Gorbushin et al. (2020) and Eremeyev, Rosi, and Naili (2020). Similar to surface elasticity phenomenon can be observed using atomistic models by Eremeyev and Sharma (2019) where the correspondence between Gurtin–Murdoch model and square lattice dynamics.

The surface elasticity is also closely related to a nonlocal models of continuum as stress and strain gradient elasticity, see Mindlin (1965), Eremeyev, Rosi, and Naili (2019) and Li, Lin, and Ng (2020). Considering non-local phenomena and surface waves it is worth to mention here the analysis performed by Chebakov, Kaplunov, and Rogerson (2016) and Gorbushin and Mishuris (2016).

The presence of such surface microstructure may essentially affected the effective material properties, stress concentration in the vicinity of crack tip, etc. Obviously, surface microstructure may also change the condition of surface waves propagation. For example, in the case of the linear Gurtin–Murdoch model and its generalization there exist surface anti-plane waves which are in the classic elasticity, see Eremeyev, Rosi, and Naili (2016), Eremeyev (2020) and Zhu, Pan, Qian, and Wang (2019) for layered structures.

Considering propagation of surface waves for curved surfaces it is worth to note initial works in the field by Babich and Rusakova (1963), Gregory (1966) and Rulf (1969), see also recent review by Kaplunov and Prikazchikov (2017). Let us also note that curved and corrugated surfaces lyes also in the focus of interests of the electromagnetism theory as they found various applications, see *e.g.* antennas design (Volakis, 2007). Under certain assumptions the governing equations of the electromagnetic theory could coincide with the equations of acoustics, see original paper by Auld, Gagnepain, and Tan (1976).

Let us note that in the most results related to surface elasticity authors consider an ideal surface as a plane, circle, cylinder, etc. In the framework of lattice dynamics it was shown that the presence of surface or interfacial imperfection may significantly change the picture of wave transmission, reflection and leakage, see, *e.g.*, Sharma (2015), Sharma (2017), Sharma (2020), Mishuris, Movchan, and Slepyan (2007), Mishuris, Movchan, and Slepyan (2009), Sharma and Eremeyev (2019), Lal Sharma and Mishuris (2020) and Nieves, Carta, Pagneux, and Brun (2020). Different types of surface imperfections were considered by Mishuris et al. (2006), Mishuris et al. (2010) and Mishuris, Movchan, and Slepyan (2020). Eremeyev (2020) proposed a homogeneous model for a surface/interface with highly anisotropic properties. Another property of any surface considered at small scales is its roughness. Indeed, a roughness of a real surface or interface constitutes an almost unavoidable property and be reached only in few rare cases. Considering a surface roughness the static analysis of stress concentration was performed by Grekov and Kostyrko (2015, 2016) and Kostyrko, Grekov, and Altenbach (2019), contact problems and cross-property connections are studied by Sevostianov and Kachanov (2009), Sevostianov and Kachanov (2007), Sevostianov and Kachanov (2020), Kuzkin and Kachanov (2015) and Lapin, Kuzkin, and Kachanov (2019), where other references could be found.

In contrast to the aforementioned papers on propagation of harmonic shear surface waves, the aim of this paper is to study propagation of *localized* shear surface waves considering both the Gurtin–Mindlin surface elasticity as a model of thin coating and the geometrical roughness of the surface. Let us note that the considered problem has multiple scale parameters related to surface elasticity modulus and to the magnitude of roughness. So both of them, compared to the shear modulus in the bulk and to the amplitude of an excited localized wave, respectively, can be used as small parameters that naturally invokes the application of asymptotic techniques.

The paper is organized as follows. First, following Gurtin and Murdoch (1978) and Eremeyev et al. (2016) we briefly recall the basic equations of the linear surface elasticity in the case of anti-plane shear deformations in Section 2. In Section 3 we transform the problem into dimensionless form for localized waves. The asymptotic technique to the derivation of a solution of the problem under consideration is applied in Section 4. Here we used the technique developed in the dynamic theory of linear elastic shells by Mikhasev (1996, 1998) and summarized by Mikhasev and Tovstik (2020). As a result, we obtain a solution which describes a surface wave localized in the vicinity of a moving front and estimate its decay rate as a function of roughness magnitude. Section 5 presents few examples of such dependence.

2. Antiplane deformations in the framework of Gurtin–Murdoch surface elasticity

Let us consider a three-dimensional elastic half-space with rough surface given by $y \leq \eta(x)$, where x, y, z are Cartesian coordinates, and $\mathbf{i}_k$, $k = 1, 2, 3$, are the unit base vectors, as shown in Fig. 1. On the free boundary $y = \eta(x)$ we assume the action of surface stresses described within the model of surface elasticity by Gurtin and Murdoch (1975, 1978).

For anti-plane deformations the vector $\mathbf{u}$ of displacements takes a simple form, see, *e.g.*, Achenbach (1973),

$$\mathbf{u}(x, y, t) = u(x, y, t)\mathbf{i}_3. \tag{1}$$

For (1) we get the formulae

$$\nabla \mathbf{u} = \left(\mathbf{i}_1 \frac{\partial u}{\partial x} + \mathbf{i}_2 \frac{\partial u}{\partial y} \right) \otimes \mathbf{i}_3, \tag{2}$$
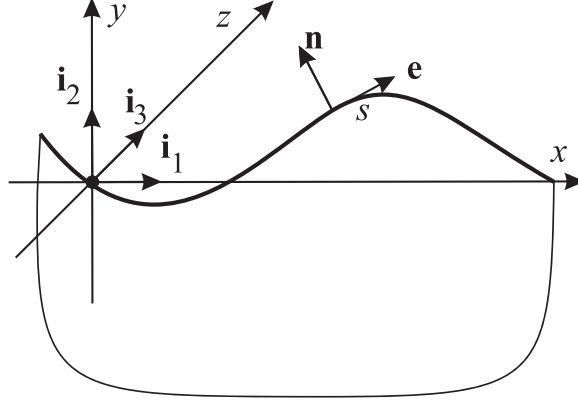
Fig. 1. Half-space with rough surface described by equation $y = \eta(x)$.

$$\boldsymbol{\varepsilon} = \frac{1}{2}\left(\nabla\mathbf{u} + (\nabla\mathbf{u})^T\right) = \varepsilon_{xz}(\mathbf{i}_1 \otimes \mathbf{i}_3 + \mathbf{i}_3 \otimes \mathbf{i}_1) + \varepsilon_{yz}(\mathbf{i}_2 \otimes \mathbf{i}_3 + \mathbf{i}_3 \otimes \mathbf{i}_2),$$

$$\varepsilon_{xz} = \frac{1}{2}\frac{\partial u}{\partial x}, \quad \varepsilon_{yz} = \frac{1}{2}\frac{\partial u}{\partial y}. \tag{3}$$

Hereinafter ∇ is the three-dimensional nabla-operator, $\otimes$ stands for the dyadic product, and T denotes the transpose operation.

In the following we consider a homogeneous medium. For an isotropic material using Hooke's law we introduce the stress tensor

$$\boldsymbol{\sigma} = 2\mu\boldsymbol{\varepsilon} = \sigma_{xz}(\mathbf{i}_1 \otimes \mathbf{i}_3 + \mathbf{i}_3 \otimes \mathbf{i}_1) + \sigma_{yz}(\mathbf{i}_2 \otimes \mathbf{i}_3 + \mathbf{i}_3 \otimes \mathbf{i}_2),$$

$$\sigma_{xz} = 2\mu\varepsilon_{xz}, \quad \sigma_{yz} = 2\mu\varepsilon_{yz}, \tag{4}$$

where μ is a constant shear modulus. As a result, the equation of motion for $x \in \mathbb{R}, y < \eta(x)$ takes the form of the wave equation

$$\mu\left(\frac{\partial^2 u}{\partial x^2} + \frac{\partial^2 u}{\partial y^2}\right) = \rho\frac{\partial^2 u}{\partial t^2}, \tag{5}$$

where ρ is a mass density.

Within the linear Gurtin-Murdoch model we introduce at the free surface $y = \eta(x)$ the surface stress tensor $\boldsymbol{\tau}$ as a linear function of surface strains $\boldsymbol{\epsilon}$. Here we have the following relations for the normal $\mathbf{n}$ and tangent $\mathbf{e}$ vectors as well as the surface nabla-operator ∇_s in the case of anti-plane deformations

$$\mathbf{e} = \frac{1}{\sqrt{1 + \eta'^2}}\left(\mathbf{i}_1 + \eta'\mathbf{i}_2\right), \tag{6}$$

$$\mathbf{n} = \frac{1}{\sqrt{1 + \eta'^2}}\left(-\eta'\mathbf{i}_1 + \mathbf{i}_2\right), \tag{7}$$

$$\nabla_s = \mathbf{e}\frac{\partial}{\partial s}, \tag{8}$$

where the prime stands for the derivative with respect to x and s is the arc-length parameter. With these formulae we get the surface strain tensor

$$\boldsymbol{\epsilon} = \frac{1}{2}\frac{\partial u}{\partial s}(\mathbf{e} \otimes \mathbf{i}_3 + \mathbf{i}_3 \otimes \mathbf{e}). \tag{9}$$

So the surface stress tensor is given by

$$\boldsymbol{\tau} = 2\mu_s\boldsymbol{\epsilon}, \tag{10}$$

where μ_s is a surface shear modulus.

The general compatibility condition at a free surface has the form (Eremeyev et al., 2016)

$$\mathbf{n} \cdot \boldsymbol{\sigma} = \nabla_s \cdot \boldsymbol{\tau} - m\frac{\partial^2 \mathbf{u}}{\partial t^2} \quad \text{at} \quad y = \eta(x), \tag{11}$$

where "·" means the scalar product and a surface density m is introduced as in Gurtin and Murdoch (1978). For anti-plane deformations, Eq. (11) transforms into the scalar equation

$$\frac{\mu}{\sqrt{1+\eta'^2}}\left(-\eta'\frac{\partial u}{\partial x}+\frac{\partial u}{\partial y}\right)=\mu_s\frac{\partial^2 u}{\partial s^2}-m\frac{\partial^2 u}{\partial t^2} \quad \text{at} \quad y=\eta(x), \tag{12}$$

where $\frac{\partial}{\partial s}$ relates to $\frac{\partial}{\partial x}$ as follows

$$\frac{\partial}{\partial s}=\frac{1}{\sqrt{1+\eta'^2}}\frac{\partial}{\partial x}.$$

For localized deformations the boundary condition (12) should be supplemented by the condition at infinity:

$$u \to 0 \quad \text{at} \quad y \to -\infty. \tag{13}$$

3. Setting the problem

For the flat boundary, i.e. when $\eta = 0$, the solution of the boundary-value problem Eqs. (5), (12) and (13) is given by Eremeyev et al. (2016) as follows

$$u = u_0\exp[\alpha y+ik(x-ct)], \quad i=\sqrt{-1}, \tag{14}$$

where u_0 is a amplitude, k is a wave number, $c = \omega/k$ is the phase velocity, and ω is the circular frequency with parameters k, c, α satisfying the following relations, see Eremeyev et al. (2016) for details,

$$\alpha^2 = k^2\left(1-\frac{c^2}{c_T^2}\right), \quad \alpha = \frac{\mu_s}{\mu}k^2\left(\frac{c^2}{c_s^2}-1\right). \tag{15}$$

Here, $c_T = \sqrt{\mu/\rho}$ is the shear wave speed in an elastic medium, and $c_s = \sqrt{\mu_s/m}$ is the shear wave speed in the thin film associated with the Gurtin–Murdoch model.

Function (14) specifies the stationary anti-plane wave, which is harmonic with respect to a coordinate x. Such waves should be treated as an idealized mathematical model describing the response of a half-space to special harmonic emitters on the entire surface. Here we consider another class of antiplane waves which can be characterized by a short wavelength and strong localization near a moving plane front given by $x = q(t)$, where $q(t)$ is an unknown function.

Let $u_0 = \max\limits_{-\infty<x<\infty} u(x,0,0)$ be the maximum amplitude of an initial wave excited in the vicinity of the line $\{x = 0, y = 0\}$. In the what follows, we consider u_0 as the characteristic length-scale parameter. Considering short-length waves, we introduce a small parameter $\varepsilon = 1/k = l/(2\pi u_0)$, where l be a wave length. We assume also that

$$\frac{m}{\rho u_0} = \varepsilon\kappa_1, \quad \frac{\mu_s}{\mu u_0} = \varepsilon\kappa_2, \quad \kappa_1,\kappa_2 \sim 1. \tag{16}$$

Estimations (16) are justified by calculations performed for a wide range of variation of u_0, l and different materials considered by Gurtin and Murdoch (1975), Gurtin and Murdoch (1978), Duan et al. (2008) and Wang et al. (2011). For instance, for the free iron surface, $m/\rho \approx 10^{-9}$m, $\mu_s/\mu \approx 3.57 \times 10^{-11}$m. It is seen that for iron $\kappa_2 < \kappa_1$ under holding the condition $\kappa_1 \sim 1$. However, in the general case, in order to take into account the effect of the surface shear modulus μ_s, we assume (16) for both κ_1 and κ_2.

Performing scaling along the y-axis, we introduce dimensionless coordinates and the maximum deflection of the rough surface from the plane as follows

$$\zeta = \frac{y}{\varepsilon u_0}, \quad \tilde{x} = \frac{x}{u_0}, \quad \eta_m = \max\limits_{-\infty<x<\infty}\eta(x). \tag{17}$$

With the dimensionless coordinates, the rough surface is defined as $\zeta = (\varepsilon u_0)^{-1}\eta_m\tilde{\eta}(u_0\tilde{x})$.

It is obvious that the dynamic characteristics of an excited wave depend on possible relations between parameters l, u_0, η_m and on a variability of the function $\eta(x)$. Varying the basic initial length-scale parameters, that are u_0 and l, we obtain possible variants of the dynamic response of the half-space to the initial wave perturbations on the surface. In particular, one can consider the following two cases as $\varepsilon \to 0$:

$$\text{A)} \qquad \frac{\eta_m}{u_0} \sim \varepsilon, \qquad \frac{\partial\eta}{\partial x} \sim \varepsilon, \tag{18}$$

$$\text{B)} \qquad \frac{\eta_m}{u_0} \sim \varepsilon, \qquad \frac{\partial\eta}{\partial x} \sim 1. \tag{19}$$

In case A, the amplitude of surface imperfections is small with respect to the amplitude u_0 of an excited wave, but has the same order as the wavelength l; the variability of the surface roughness in the x-direction is small so that its characteristic length (e.g., a period if $\eta(x)$ is a periodic function) has the order ε^{-1}. In case B, the second estimate means that the variability of the surface imperfection is of the same order as the wavelength.

Here we consider case A and assume that $\eta_m/u_0 = \varepsilon r$, where $r \sim 1$. Then we introduce new function for the roughness $f(\tilde{x}) = r\tilde{\eta}(u_0\tilde{x})$, and so $\partial f/\partial \tilde{x} \sim 1$.

In the following we consider a traveling surface wave localized near a moving plane $\tilde{x} = q(\tau)$, where $q(\tau)$ is an unknown twice differentiable function of dimensionless time τ and $q(0) = 0$. Here we define τ as $\tau = \omega_c t$, where $\omega_c = c_T/u_0$ is the characteristic frequency. We introduce the local coordinate ξ in the neighbourhood of $\tilde{x} = q(\tau)$ as follows

$$\tilde{x} = q(\tau) + \varepsilon^{1/2}\xi, \tag{20}$$

After changing coordinate $\tilde{x} \to \xi$, Eq. (5) takes the following form:

$$\varepsilon \frac{\partial^2 u}{\partial \xi^2} + \frac{\partial^2 u}{\partial \zeta^2} - \varepsilon^2 \frac{\partial^2 u}{\partial \tau^2} + 2\varepsilon^{3/2}\dot{q}\frac{\partial^2 u}{\partial \xi \partial \tau} + 2\varepsilon^{3/2}\ddot{q}\frac{\partial u}{\partial \xi} - \varepsilon \dot{q}^2 \frac{\partial^2 u}{\partial \xi^2} = 0, \tag{21}$$

and the boundary condition (12) reads

$$\frac{1}{\sqrt{1 + \varepsilon^2 f'^2}}\left(-\varepsilon^{3/2} f'^2 \frac{\partial u}{\partial \xi} + \frac{\partial u}{\partial \zeta}\right) - \varepsilon \frac{\kappa_2}{\sqrt{1 + \varepsilon^2 f'^2}}\frac{\partial}{\partial \xi}\left(\frac{1}{\sqrt{1 + \varepsilon^2 f'^2}}\frac{\partial u}{\partial \xi}\right)$$

$$+ \kappa_1\left(\varepsilon^2 \frac{\partial^2 u}{\partial \tau^2} - 2\varepsilon^{3/2}\dot{q}\frac{\partial^2 u}{\partial \xi \partial \tau} - 2\varepsilon^{3/2}\ddot{q}\frac{\partial u}{\partial \xi} + \varepsilon \dot{q}^2 \frac{\partial^2 u}{\partial \xi^2}\right) = 0 \quad \text{at} \quad \zeta = f(\tilde{x}), \tag{22}$$

where the function $f(\tilde{x})$ is expanded into the series

$$f(\tilde{x}) = f[q(\tau)] + \varepsilon^{1/2} f'[q(\tau)]\xi + \frac{1}{2}\varepsilon f''[q(\tau)]\xi^2 + \dots \tag{23}$$

in the neighbourhood of the moving plane $\tilde{x} = q(\tau)$.

Introducing the additional condition

$$u(\xi, \zeta, \tau; \varepsilon) \to 0 \quad \text{at} \quad \zeta \to -\infty, \tag{24}$$

we arrive to the boundary-value problem (21), (22) and (24), which describes the propagation of localized anti-plane waves running in the x-direction and decaying with the depth of the half-space.

4. Asymptotic solution

We shall seek a solution of the boundary-value problem (21), (22) and (24) in the form of the following asymptotic series (Mikhasev, 1996; 1998)

$$u(\zeta, \xi, \tau; \varepsilon) = \sum_{j=0}^{\infty} u_j(\zeta, \xi, \tau) \exp\left\{i\varepsilon^{-1}S(\xi, \tau.\varepsilon)\right\},$$

$$S(\xi, \tau; \varepsilon) = \int_0^{\tau} \omega(\tau')d\tau' + \varepsilon^{1/2} p(\tau)\xi + \frac{1}{2}\varepsilon b(\tau)\xi^2, \tag{25}$$

where $\omega(\tau)$, $p(\tau)$, $b(\tau)$ are twice differentiable functions of τ and $u_j(\zeta, \xi, \tau; \varepsilon)$ are polynomials in ξ with complex-valued coefficients which are twice differentiable with respect to ξ, ζ and τ, and satisfy the following conditions:

$$\Im b(\tau) > 0 \quad \text{for any} \quad \tau \geq 0, \tag{26}$$

$$\{Y, \partial Y/\partial \varsigma\} = O(1) \quad \text{as} \quad \varepsilon \to 0. \tag{27}$$

Here $\Im b$ denotes the imaginary part of the complex-valued function $b(\tau)$, Y is any of functions ω, p, b, u_j, and ς is any of their arguments. All the introduced functions appearing in (25) have the specific mechanical sense. In particular, $\omega(\tau)$ is the instantaneous frequency, the real wave parameter $p(\tau)$ determines the variability of waves in the x- direction, $\varepsilon^{-1}p$ is a wave number, and $b(\tau)$ with the positive imaginary part, see (26), characterizes the decay rate of the wave amplitudes far away from the moving plane $\tilde{x} = q(\tau)$.

In contrast to (14), the asymptotic expansion of a solution in the form of (25) allows one to describe the propagation of localized waves. For the first time, this ansatz has been proposed by Mikhasev (1996) to study localized waves traveling in the circumferential direction in thin elastic non-circular cylindrical shells with arbitrary edges. In the above paper, a solution similar to (25) was called the wave packet (WP) with the centre on the line at which amplitudes reach the maximum (here it is $\tilde{x} = q(\tau)$). Later this method was successfully applied to predict localized bending, longitudinal and torsional waves running in the axial direction in infinite cylindrical shells subjected to a dynamic normal pressure by Mikhasev (1998) and to an axial compression by Avdoshka and Mikhasev (2001).

In order to determine introduced functions, we substitute (25) into (21) and boundary conditions (22) and (24). Equating coefficients by the same powers of $\varepsilon^{1/2}$, one arrives at the sequence of differential equations

$$\sum_{m=0}^{j} \mathbf{L}_m u_{j-m} = 0, \quad j = 0, 1, 2, \dots, \tag{28}$$

where

$$\mathbf{L}_0 = \frac{\partial^2}{\partial \zeta^2} - p^2 + (\omega - \dot{q}p)^2,$$

$$\mathbf{L}_1 = (b\mathbf{L}_p + \dot{p}\mathbf{L}_\omega)\xi - i\mathbf{L}_p \frac{\partial}{\partial \xi},$$

$$\mathbf{L}_2 = \tfrac{1}{2}\left(b^2\mathbf{L}_{pp} + \dot{p}^2\mathbf{L}_{\omega\omega} + 2\dot{p}b\mathbf{L}_{\omega p} + \dot{b}\mathbf{L}_\omega\right)\xi^2 \tag{29}$$

$$-\frac{1}{2}\mathbf{L}_{pp}\frac{\partial^2}{\partial \xi^2} - i(b\mathbf{L}_{pp} + \dot{p}\mathbf{L}_{\omega p})\xi\frac{\partial}{\partial \xi} - i\mathbf{L}_\omega\frac{\partial}{\partial t} - i\left(\frac{1}{2}b\mathbf{L}_{pp} + \frac{1}{2}\dot{\omega}\mathbf{L}_{\omega\omega} + \dot{p}\mathbf{L}_{\omega p} + \ddot{q}p\right), \dots,$$

and the sequence of boundary conditions

$$\sum_{m=0}^{j} \mathbf{G}_m u_{j-m} = 0 \quad \text{at} \quad \zeta = f[q(t)],$$
$$u_j \to 0 \quad \text{as} \quad \zeta \to -\infty, \quad j = 0, 1, 2, \dots \tag{30}$$

with the operators

$$\mathbf{G}_0 = \frac{\partial}{\partial \zeta} + p^2 - \kappa(\omega - \dot{q}p)^2,$$

$$\mathbf{G}_1 = \frac{\partial \mathbf{G}_0}{\partial \zeta}f'(q)\xi + \mathbf{L}_1,$$

$$\mathbf{G}_2 = \frac{1}{2}\frac{\partial^2 \mathbf{G}_0}{\partial \zeta^2}f''(q)\xi^2 + \mathbf{L}_2 + f'^2(q)p, \dots \tag{31}$$

Hereinafter indices p, q, ω mean differentiation with respect to the corresponding variables, and the overdot denotes the derivative with respect to τ.

All required functions from ansatz (25) can be found by the consequent consideration of the boundary-value problems (28) and (30). The general asymptotic procedure is described by Mikhasev and Tovstik (2020) in all details. Here we restrict ourselves to consideration of the principal steps.

In the leading approximation, *i.e.* at $j = 0$, one has the homogeneous boundary-value problem (28) and (30). It has the non-trivial solution

$$u_0 = P_0(\xi, \tau)z_0(\zeta, q), \quad z_0 = e^{\alpha(p)\{\zeta - f[q(\tau)]\}}, \tag{32}$$

where

$$\alpha(p) = \frac{\sqrt{1 + 4\kappa_1(\kappa_1 - \kappa_2)p^2} - 1}{2\kappa_1}, \tag{33}$$

if

$$\omega = \dot{q}p \mp H(p), \tag{34}$$

where $H(p)$ is the Hamilton function defined as

$$H = \sqrt{p^2 - \alpha^2(p)}. \tag{35}$$

In (32), $P_0(\xi, \tau)$ is a polynomial in ξ with complex-valued coefficients dependent of τ, in general. Related to $\pm$ sign the non-uniqueness in the formula for ω is associated with the presence of two branches of a solution corresponding to waves propagating in two opposite directions.

It is seen that the function $z_0(\zeta, \tau)$ decays if $\kappa_1 > \kappa_2$, that is justified by above calculations for iron as well as for other materials. This inequality is equivalent to the condition by Eremeyev et al. (2016) and is given by $c_s < c_T$.

In the first-order approximation ($j = 1$), we arrive at the inhomogeneous boundary-value problem (28) and (30). The compatibility condition of this problem reads

$$\int_{-\infty}^{f(q)} (\mathbf{L}_0 u_1 + \mathbf{L}_1 u_0)z_0 \, d\zeta = 0. \tag{36}$$

Taking into account relations (32) and (34), this condition can be rewritten as the differential equation

$$i(\dot{q} - H_p)\frac{\partial P_0}{\partial \xi} + \dot{p}\xi P_0 - b(\dot{q} - H_p)\xi P_0 = 0. \tag{37}$$

with respect to $P_0(\xi)$. Note that by our assumptions, $\Im b(\tau) > 0$ for any $\tau \geq 0$. Hence, Eq. (37) has a solution in the form of polynomials if and only if the unknown functions satisfy the equations

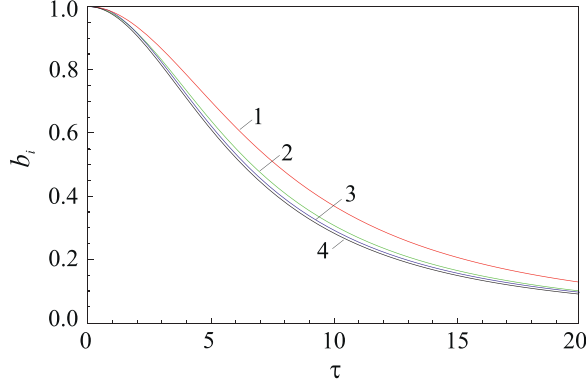$$\dot{q} = \pm H_p, \quad \dot{p} = 0. \tag{38}$$

Fig. 2. Parameter $b_i = \Im b$ vs. dimensional time τ for fixed $p = 1.0, \kappa_2 = 0$ and different values of a parameter κ_1: 1 - $\kappa_1 = 0.6$; 2 - $\kappa_1 = 0.8$; 3 - $\kappa_1 = 1.0$; 4 - $\kappa_1 = 1.2$.

Then $q(\tau) = H_p \tau$ is the linear function of time, and the wave parameter $p = p^\circ$ is a constant. As a consequence, the instantaneous circular frequency

$$\omega = |\pm p^\circ H_p(p^\circ) \mp H(p^\circ)| \tag{39}$$

has also a constant value. Relation (39) coincides with the dispersion equation followed from (15) for a plane surface (Eremeyev et al., 2016).

Thus, under the aforementioned assumptions with respect to the wavelength and all parameters of the problem, a smooth imperfection of the surface, characterized by the function $\eta(x)$, does not effect such dynamic parameters of localized anti-plane waves as the wave number p, the group velocity $v_g = H_p$ and the circular frequency ω. On the other hand, it influences the function

$$z_0(\zeta, \tau) = e^{\alpha(p)\{\zeta - f[H_p(p)\tau]\}}, \tag{40}$$

which determines the depth of waves penetration in a half-space along the moving plane $x = u_0[\omega_c H_p(p)t + \varepsilon^{1/2}\xi]$.

Accounting for Eqs. (38), the solution of the boundary-value problem (28) and (30) for $j = 1$ can be written as $u_1 = P_1(\xi, \tau)z_0(\zeta, q)$, where P_1 is a polynomial in ξ which together with P_0 remains undefined at this step.

Let us now consider the second-order approximation. It generates again the inhomogeneous boundary-value problem (28) and (30) for $j = 2$. Omitting for brevity awkward transformations, we come to in the following differential equation with respect to P_0, see Mikhasev and Tovstik (2020)) for more details

$$h\left(\frac{\partial^2 P_0}{\partial \xi^2} - 2ib\xi \frac{\partial P_0}{\partial \xi}\right) - \left[hb^2 + H(1 + 2\kappa_1\alpha)b\right]\xi^2 P_0$$
$$+ 2iH(1 + 2\kappa_1\alpha)\frac{\partial P_0}{\partial \tau} + i\left[hb + 2\alpha p f'^2(q)\right]P_0 = 0, \tag{41}$$

where

$$h = h(p) = 1 + 2\kappa_2\alpha(p) - [1 + 2\kappa_1\alpha(p)]H_p^2(p). \tag{42}$$

Eq. (41) has a solution in the polynomial form with respect to ξ if and only if

$$\dot{b} + F(p)b^2 = 0, \quad F(p) = \frac{h(p)}{[1 + 2\kappa_1\alpha(p)]H(p)}. \tag{43}$$

Hence, one obtains

$$b(\tau) = \frac{b^\circ}{1 + b^\circ F(p)\tau}, \tag{44}$$

where $b^\circ = b(0)$ is the initial value of the complex-valued function $b(\tau)$.

One can prove that if $\kappa_1 > \kappa_2$, then $F(p) > 0$ for any wave parameter p. Then $\Im b(\tau) > 0$ and $\Im \dot{b}(\tau) < 0$ for any finite time interval. These inequalities mean that an excited localized anti-plane surface wave spreads during time, at that the rate of spreading depends strongly on the wave parameter p and parameters κ_1, κ_2 as well. It can be readily proved that the width of an excited wave packet is a monotonically decreasing function of a wave parameter p. In Fig. 2, the function $b_i = \Im b(\tau)$ is depicted for the fixed $p = 1.0$, $\kappa_2 = 0$ and different values of a parameter $\kappa_1 = 0.6, 0.8, 1.0, 1.2$. It is seen that the wave packet width increases with time and is a weakly increasing function of κ_1. Fig. 3 shows the same function $b_i = \Im b(\tau)$ versus time under fixed values $p = 1, \kappa_1 = 1$ and different values $\kappa_2 = 0, 0.2, 0.4, 0.6$. One can see an interesting effect: function $\Im b(\tau)$ increases together with parameter $\kappa_2 = \mu_s/(u_0\mu)$. In other words, an increase in the surface shear modulus decelerates the process of "crawling" the packet of anti-plane waves away over the surface.
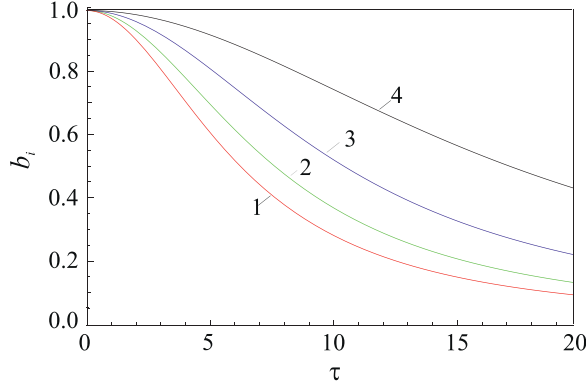
Fig. 3. Parameter $b_i = \Im b$ vs. dimensional time τ for fixed $p = 1.0$, $\kappa_1 = 1.0$ and different values of a parameter κ_2: 1 - $\kappa_2 = 0$; 2 - $\kappa_2 = 0.2$; 3 - $\kappa_2 = 0.4$; 4 - $\kappa_2 = 0.6$.

Let us come back to Eq. (41). Taking relation (44) into account, we arrive at the amplitude equation with respect to $P_0(\xi, \tau)$:

$$a_2 \frac{\partial^2 P_0}{\partial \xi^2} + a_1 \xi \frac{\partial P_0}{\partial \xi} + \frac{\partial P_0}{\partial \tau} + a_0 P_0 = 0, \tag{45}$$

where

$$a_0 = \frac{1}{2} b(\tau) F + \frac{\alpha p f'^2(H_p \tau)}{(1 + 2\kappa_1 \alpha) H}, \quad a_1 = bF, \quad a_2 = -\frac{i}{2} F. \tag{46}$$

A solution of Eq. (45) can be expressed in terms of Hermite polynomials with coefficients depending on time, see Mikhasev (2002). Here we give the simplest representation of a required solution as in Mikhasev and Tovstik (2020),

$$P_0 = \sum_{n=0}^{N} A_n(\tau) \xi^n. \tag{47}$$

with $A_n(\tau)$ defined from the following recurrence relations:

$$A_N = c_N \Psi_N(\tau), \quad A_{N-1} = c_{N-1} \Psi_{N-1}(\tau),$$

$$A_{N-r} = \Psi_{N-r}(\tau) \left[c_{N-r} - (N-r+2)(N-r+1) \int_0^\tau \frac{a_2(\tau) A_{N-r+2}(\tau)}{\Psi_{N-r}(\tau)} d\tau \right], \tag{48}$$

$$\Psi_n(\tau) = \exp\left\{ -\int_0^\tau [n a_1(\tau) + a_0(\tau)] d\tau \right\},$$

where c_n are arbitrary complex constants to be determined from the initial conditions, and $r = 2, 3, N$; $n = 0, 1, \ldots, N$.

In particular, for $N = 0$ we obtain,

$$P_0(\tau) = \frac{c_0}{\sqrt{1 + b^\circ F(p) \tau}} \exp\left\{ -\frac{\alpha(p) p}{[1 + 2\kappa_1 \alpha(p)] H(p)} \int_0^\tau f'^2[H_p(p)\tau] d\tau \right\}. \tag{49}$$

It is clear that if f is a constant, then the maximum amplitude of the localized anti-plane waves is a monotonically decreasing function of time. If not, it reveals a complicated behaviour *versus* time, which is affected by the form of surface imperfection. However, regardless of the function $f(\tilde{x})$, one can conclude that $\lim_{\tau \to \infty} P_0(\tau) = 0$, *i.e.*, these waves spread over the surface and decay during time.

5. Example and discussion

Let the surface imperfection be given by the periodic function $f(\tilde{x}) = f_0 \sin \delta \tilde{x}$, where $f_0 \sim 1$, $\delta \sim 1$. Fig. 4 displays the maximum amplitude $A_m = \Re P_0(\tau)$ of waves at the rough surface *versus* dimensionless time τ for $c_0 = 1$, $p = p^\circ = 1$, $\delta = 1$, $b^\circ = i$, $\kappa_1 = 1$, $\kappa_2 = 0$ at different values of a parameter $f_0 = 0, 0.5, 1.0, 1.5$. Here $\Re$ denotes the real part of a complex-valued function. One can see that for a plane surface ($f_0 = 0$) the maximum amplitude is a smoothly decreasing function of time, and the presence of roughness distorts the function $A_m = \Re P_0(\tau)$, and this distortion being the stronger, the greater the amplitude of the surface roughness. Also, an increase in the roughness height leads to a faster decay of the amplitude of localized anti-plane waves.
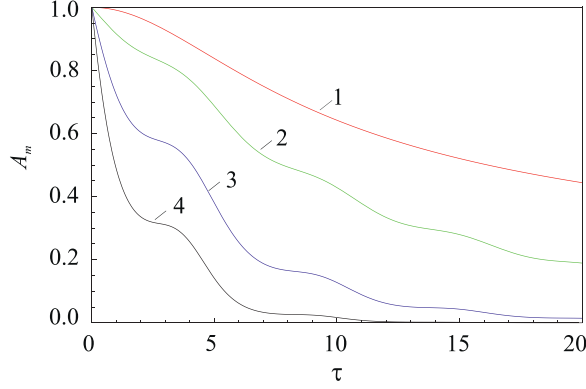
Fig. 4. The maximum amplitude $A_m = \Re P_0(\tau)$ vs. dimensional time τ for different values of a parameter f_0: 1 - $f_0 = 0$; 2 - $f_0 = 0.5$; 3 - $f_0 = 1.0$; 4 - $f_0 = 1.5$.
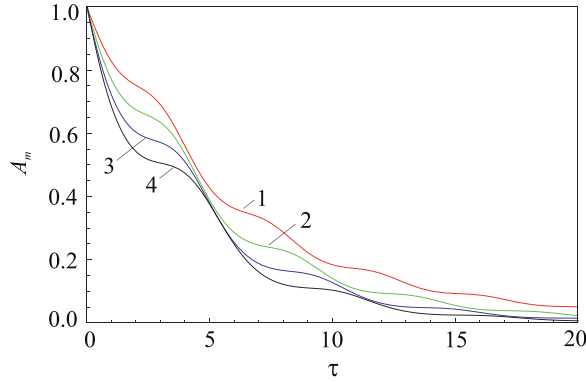

Fig. 5. The maximum amplitude $A_m = \Re P_0(\tau)$ vs. dimensional time τ for different values of a wave parameter p: 1 - $p = 0.6$; 2 - $p = 0.8$; 3 - $p = 1.0$; 4 - $p = 1.2$.

Calculations of $A_m = \Re P_0(\tau)$ for the fixed $f_0 = 1$ and different wave parameters p with the remaining parameters being as in the previous example revealed unexpected effect (see Fig. 5): an increase in the wave parameter (*i.e.*, a decrease in the wavelength) entails a more rapid decrease in the amplitude of anti-plane localized waves. We note that the Hamilton function $H(p)$ can be treated as "an energy" of the initial wave packet, which is the monotonically increasing function of p. The study of wave packets in thin shells of medium length has showed the fairly expected result: the WP amplitude decays the slower, the higher its "initial energy", see Mikhasev and Tovstik (2020). In our case, the opposite effect can be explained by an increase of the function $\alpha(p)$ together with the wave parameter p, see Eq. (33). We remind that the function $\alpha(p)$ determines the depth of wave penetration with distance from the surface $\zeta = f(\tilde{x})$. Growing the parameter p results in increasing that part of energy which is dissipated at the depth of the half-space and far from the moving plane $\tilde{x} = q(\tau)$. The corresponding relation for an estimation of the maximum amplitude A_d of waves at a depth $d > 0$ from any point of the rough surface reads

$$A_d = A_m(\tau)e^{-\alpha(p)d}. \tag{50}$$

From this relation and Figs. 4 and 5 it can be seen that for any fixed time instant, the wave amplitude decaying exponentially with the depth. Eq. (33) shows that $\alpha(p; \kappa_1, \kappa_2)$ is a monotonically increasing function of parameters p, κ_1 and a decreasing function of κ_2. Hence, one can conclude that the rate of waves attenuation with a distance from the surface grows together with the wave parameter p and the surface density m for fixed other parameters (ρ, μ, μ_s, u_0), and contrary, it drops when $\mu_s/(u_0\mu)$ increases.

The outcomes of computations of the amplitude $A_m = \Re P_0(\tau)$ at the rough surface for $\kappa_1 = 1$ and different values of the shear parameter $\kappa_2 = 0; 0.2; 0.4; 0.6$ are shown in Fig. 6. Other parameters are as in the first example. It is seen that the rate of decay of the amplitude of localized anti-plane waves during time is strongly affected by the surface shear modulus μ_s; it grows as a parameter κ_2 decreases. For instance, for the free iron surface with very small ratio $\mu_s/\mu \approx 3.57 \times 10^{-11}$m, we can assume $\kappa_2 \approx 0$, if the initial amplitude u_0 is such that the asymptotic estimate $\kappa_1 \sim 1$ holds. However, if we consider a free surface with a thin near-surface layer for which $\mu_s = \mu_{ns}h_{ns}$, where μ_{ns} is the shear modulus of material of the near-surface layer of the thickness h_{ns}, see Mishuris et al. (2006) and Eremeyev et al. (2020), then by varying the thickness h_{ns}, one can obtain a non-zero ratio $\kappa_2 < \kappa_1$. Obviously, in the first case (for a free surface of iron film) the localized anti-plane
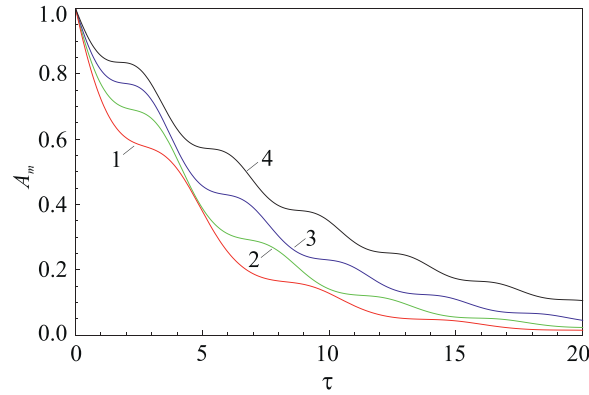
Fig. 6. The maximum amplitude $A_m = \Re P_0(\tau)$ *vs.* dimensional time τ for different values of a shear parameter κ_2: 1 - $\kappa_2 = 0$; 2 - $\kappa_2 = 0.2$; 3 - $\kappa_2 = 0.4$; 4 - $\kappa_2 = 0.6$.

waves decay faster than in the second one (for a free surface with a thin near-surface layer of finite thickness). It is worth to emphasized once more that a decrease in the surface shear modulus μ_s in comparison with $u_0\mu$, where μ is the shear modulus in a bulk and u_0 is the initial amplitude of localized waves, leads to an increase in the decay rate of localized waves on the corrugated surface and to a decrease of this rate at the depth of the half-plane far from the surface.

We note that the performed analysis of localized shear surface waves is related to case A corresponding to a small variation of the surface roughness in the *x*-direction. It may be considered as a benchmark solution for subsequent detailed investigations of other possible relations between the main parameters of the problem (l, u_0, η_m) including case B.

6. Conclusions

We discussed the propagation of localized surface waves in an elastic half-space with a thin coating modeled through the linear Gurtin–Murdoch surface elasticity. The main aim of the paper was to analyze a roughness influence on the wave localization. We modeled roughness as a geometric deviation from the flat surface. Let us note that from engineering point of view roughness is an almost unavoidable property of any surface and should be taken into account for the analysis of surface waves. The latter are widely used in modern engineering, for example, as carriers of an information on surface defects and other material properties in a vicinity of a surface. In this paper we applied the asymptotic approach developed earlier for elastic shells (Mikhasev, 1996; 1998; Mikhasev & Tovstik, 2020). The obtained solution and performed calculations allow us to conclude that:

- the effect of surface roughness on the localized wave characteristics essentially depends on the following parameters: the initial wave amplitude/wavelength ratio, the correlations between the surface density and material density in the bulk, the surface shear modulus and shear modulus of the near-surface layer, the amplitude of surface imperfection and the initial wave amplitude, and the roughness characteristic length as well;
- the smooth roughness of small amplitude does not affect the wave number, instantaneous frequency, group velocity, and width of an excited localized wave, but strongly affects its amplitude, distorting the latter over time;
- the decay rate of anti-plane localized waves at the rough surface grows when the wave number increases and/or the surface shear modulus decreases;
- the decay rate of anti-plane localized waves in depth direction increases together with the wave number and the surface density and decreases when the surface shear modulus increases.

The presented results complement previous ones for ideal plane boundary or for surface inhomogeneity presented by Eremeyev et al. (2016) and by Sharma and Eremeyev (2019), respectively. This property could be used for evaluation of surface properties using ultrasound waves techniques, as, for example, for evaluation of the stability of dental implants (Hériveaux, Nguyen, Biwa, & Haïat, 2020; Scala et al., 2018).

Declaration of Competing Interest

The authors of the paper JENS-D-20-01346 entitled "On the influence of a surface roughness on propagation of anti-plane short-length localized waves in a medium with surface coating" declare that there is no conflict of interest.

Acknowledgments

References

Achenbach, J. (1973). *Wave propagation in elastic solids*. Amsterdam: North Holland.

Auld, B. A., Gagnepain, J. J., & Tan, M. (1976). Horizontal shear surface waves on corrugated surfaces. *Electronic Letters, 12*, 650–652.

Avdoshka, I. V., & Mikhasev, G. I. (2001). Wave packets in a thin cylindrical shell under a non-uniform axial load. *Journal of Applied Mathematics and Mechanics, 65*, 301–309.

Babich, V. M., & Rusakova, N. Y. (1963). The propagation of Rayleigh waves over the surface of a non-homogeneous elastic body with an arbitrary form. *USSR Computational Mathematics and Mathematical Physics, 2*, 719–735.

Baranova, S., Mogilevskaya, S. G., Nguyen, T. H., & Schillinger, D. (2020). Higher-order imperfect interface modeling via complex variables based asymptotic analysis. *International Journal of Engineering Science, 157*, 103399.

Benveniste, Y. (2006). A general interface model for a three-dimensional curved thin anisotropic interphase between two anisotropic media. *Journal of the Mechanics and Physics of Solids, 54*, 708–734.

Benveniste, Y., & Berdichevsky, O. (2010). On two models of arbitrarily curved three-dimensional thin interphases in elasticity. *International Journal of Solids and Structures, 47*, 1899–1915.

Benveniste, Y., & Miloh, T. (2001). Imperfect soft and stiff interfaces in two-dimensional elasticity. *Mechanical Materials, 33*, 309–323.

Chebakov, R., Kaplunov, J., & Rogerson, G. A. (2016). Refined boundary conditions on the free surface of an elastic half-space taking into account non-local effects. *Proceedings of the Royal Society A: Mathematical, Physical and Engineering Sciences, 472*, 20150800.

Doan, T., Le-Quang, H., & To, Q. D. (2020). Effective elastic stiffness of 2D materials containing nanovoids of arbitrary shape. *International Journal of Engineering Science, 150*, 103234.

Duan, H. L., Wang, J., & Karihaloo, B. L. (2008). Theory of elasticity at the nanoscale. In *Adv. appl. mech.: vol. 42* (pp. 1–68). Elsevier.

Eremeyev, V. A. (2016). On effective properties of materials at the nano- and microscales considering surface effects. *Acta Mechanica, 227*, 29–42.

Eremeyev, V. A. (2020). Strongly anisotropic surface elasticity and antiplane surface waves. *Philosophical Transactions of the Royal Society A, 378*, 20190100. https://doi.org/10.1098/rsta.2019.0100.

Eremeyev, V. A., Rosi, G., & Naili, S. (2016). Surface/interfacial anti-plane waves in solids with surface energy. *Mechanics Research Communications, 74*, 8–13.

Eremeyev, V. A., Rosi, G., & Naili, S. (2019). Comparison of anti-plane surface waves in strain-gradient materials and materials with surface stresses. *Mathematics and Mechanics of Solids, 24*, 2526–2535.

Eremeyev, V. A., Rosi, G., & Naili, S. (2020). Transverse surface waves on a cylindrical surface with coating. *International Journal of Engineering Science, 147*, 103188.

Eremeyev, V. A., & Sharma, B. L. (2019). Anti-plane surface waves in media with surface structure: Discrete vs. continuum model. *International Journal of Engineering Science, 143*, 33–38.

Gorbushin, N., Eremeyev, V. A., & Mishuris, G. (2020). On stress singularity near the tip of a crack with surface stresses. *International Journal of Engineering Science, 146*, 103183.

Gorbushin, N., & Mishuris, G. (2016). Dynamic crack propagation along the interface with non-local interactions. *Journal of the European Ceramic Society, 36*, 2241–2244.

Gregory, R. D. (1966). The attenuation of a Rayleigh wave in a half-space by a surface impedance. *Mathematical Proceedings of the Cambridge Philosophical Society, 62*, 811–827.

Grekov, M. A., & Kostyrko, S. A. (2015). A multilayer film coating with slightly curved boundary. *International Journal of Engineering Science, 89*, 61–74.

Grekov, M. A., & Kostyrko, S. A. (2016). Surface effects in an elastic solid with nanosized surface asperities. *International Journal of Solids and Structures, 96*, 153–161.

Gurtin, M. E., & Murdoch, A. I. (1975). A continuum theory of elastic material surfaces. *Archievefor Rational Mechanicsand Analysis, 57*, 291–323.

Gurtin, M. E., & Murdoch, A. I. (1978). Surface stress in solids. *International Journal of Solids and Structures, 14*, 431–440.

Han, Z., Mogilevskaya, S. G., & Schillinger, D. (2018). Local fields and overall transverse properties of unidirectional composite materials with multiple nanofibers and Steigmann–Ogden interfaces. *International Journal of Solids and Structures, 147*, 166–182.

Hériveaux, Y., Nguyen, V.-H., Biwa, S., & Haïat, G. (2020). Analytical modeling of the interaction of an ultrasonic wave with a rough bone-implant interface. *Ultrasonics, 108*, 106223.

Huang, Z. P., & Wang, J. X. (2006). A theory of hyperelasticity of multi-phase media with surface/interface energy effect. *Acta Mechanica, 182*, 195–210.

Kaplunov, J., & Prikazchikov, D. A. (2017). Asymptotic theory for Rayleigh and Rayleigh-type waves. *Advances in Applied Mechanics, 50*, 1–106.

Kim, C. I., Ru, C. Q., & Schiavone, P. (2013). A clarification of the role of crack-tip conditions in linear elasticity with surface effects. *Mathematics and Mechanics of Solids, 18*, 59–66.

Kostyrko, S., Grekov, M., & Altenbach, H. (2019). Stress concentration analysis of nanosized thin-film coating with rough interface. *Continuum Mechanics and Thermodynamics, 31*, 1863–1871.

Kuzkin, V. A., & Kachanov, M. (2015). Contact of rough surfaces: Conductance?stiffness connection for contacting transversely isotropic half-spaces. *International Journal of Engineering Science, 97*, 1–5.

Lal Sharma, B., & Mishuris, G. (2020). Scattering on a square lattice from a crack with a damage zone. *Proceedings of the Royal Society A, 476*, 20190686.

Lapin, R. L., Kuzkin, V. A., & Kachanov, M. (2019). Rough contacting surfaces with elevated contact areas. *International Journal of Engineering Science, 145*, 103171.

Li, L., Lin, R., & Ng, T. Y. (2020). Contribution of nonlocality to surface elasticity. *International Journal of Engineering Science, 152*, 103311.

Mikhasev, G. I. (1996). Localized sets of bending waves in a noncircular cylindrical shell with slanted edges. *Prikladnaya Matematika i Mekhanika, 60*. 635–634

Mikhasev, G. I. (1998). Travelling wave packets in an infinite thin cylindrical shell under internal pressure. *Journal of Sound and Vibration, 209*, 543–559.

Mikhasev, G. I. (2002). Localized families of bending waves in a thin medium-length cylindrical shell under pressure. *Journal of Sound and Vibration, 253*, 833–857.

Mikhasev, G. I., & Tovstik, P. E. (2020). *Localized dynamics of thin-walled shells*. Boca Raton: CRC Press.

Mindlin, R. D. (1965). Second gradient of strain and surface-tension in linear elasticity. *International Journal of Solids and Structures, 1*, 417–438.

Mishuris, G. S., Movchan, A. B., & Slepyan, L. I. (2007). Waves and fracture in an inhomogeneous lattice structure. *Waves in Random and Complex Media, 17*, 409–428.

Mishuris, G. S., Movchan, A. B., & Slepyan, L. I. (2009). Localised knife waves in a structured interface. *Journal of the Mechanics and Physics of Solids, 57*, 1958–1979.

Mishuris, G. S., Movchan, A. B., & Slepyan, L. I. (2020). Waves in elastic bodies with discrete and continuous dynamic microstructure. *Philosophical Transactions of the Royal Society A, 378*, 20190313.

Mishuris, G. S., Movchan, N. V., & Movchan, A. B. (2006). Steady-state motion of a mode-III crack on imperfect interfaces. *The Quarterly Journal of Mechanics & Applied Mathematics, 59*, 487–516.

Mishuris, G. S., Movchan, N. V., & Movchan, A. B. (2010). Dynamic mode-III interface crack in a bi-material strip. *International Journal of Fracture, 166*, 121–133.

Murdoch, A. I. (2005). Some fundamental aspects of surface modelling. *Journal of Elasticity, 80*, 33–52.

Nieves, M. J., Carta, G., Pagneux, V., & Brun, M. (2020). Rayleigh waves in micro-structured elastic systems: Non-reciprocity and energy symmetry breaking. *International Journal of Engineering Science, 156*, 103365.

Ru, C. Q. (2010). Simple geometrical explanation of Gurtin-Murdoch model of surface elasticity with clarification of its related versions. *Science China Physics, Mechanics and Astronomy, 53*, 536–544.

Rulf, B. (1969). Rayleigh waves on curved surfaces. *The Journal of the Acoustical Society of America, 45*, 493–499.

Scala, I., Rosi, G., Nguyen, V.-H., Vayron, R., Haiat, G., Seuret, S., … Naili, S. (2018). Ultrasonic characterization and multiscale analysis for the evaluation of dental implant stability: a sensitivity study. *Biomedical Signal Processing and Control, 42*, 37–44.

Sevostianov, I., & Kachanov, M. (2007). Contacting rough surfaces: Hertzian contacts versus welded areas. *International Journal of Fracture, 145*, 223.

Sevostianov, I., & Kachanov, M. (2009). Elasticity–conductivity connections for contacting rough surfaces: An overview. *Mechanics of Materials, 41*, 375–384.

Sevostianov, I., & Kachanov, M. (2020). Evaluation of the incremental compliances of non-elliptical contacts by treating them as external cracks. *European Journal of Mechanics-A/Solids*, 104114.

Sharma, B. L. (2015). Diffraction of waves on square lattice by semi-infinite crack. *SIAM Journal on Applied Mathematics, 75*, 1171–1192.

Sharma, B. L. (2017). On scattering of waves on square lattice half-plane with mixed boundary condition. *Zeitschrift für angewandte Mathematik und Physik, 68*, 120.

Sharma, B. L. (2020). Discrete scattering by two staggered semi-infinite defects: Reduction of matrix wiener-HOPF problem. *Journal of Engineering Mathematics, 123*, 41–87.

Sharma, B. L., & Eremeyev, V. A. (2019). Wave transmission across surface interfaces in lattice structures. *International Journal of Engineering Science, 145*, 103173.

Steigmann, D. J., & Ogden, R. W. (1997). Plane deformations of elastic solids with intrinsic boundary elasticity. *Proceedings of the Royal Society A, 453*, 853–877.

Steigmann, D. J., & Ogden, R. W. (1999). Elastic surface-substrate interactions. *Proceedings of the Royal Society A, 455*, 437–474.

(2007). In J. L. Volakis (Ed.), *Antenna engineering handbook* ((4th ed.)). New York: McGrawHill.

Wang, J., Huang, Z., Duan, H., Yu, S., Feng, X., Wang, G., … Wang, T. (2011). Surface stress effect in mechanics of nanostructured materials. *Acta Mechanica Solida Sinica, 24*, 52–82.

Zemlyanova, A. Y. (2020). Interaction of multiple plane straight fractures in the presence of the Steigmann–Ogden surface energy. *SIAM Journal on Applied Mathematics, 80*, 2098–2119.

Zhu, F., Pan, E., Qian, Z., & Wang, Y. (2019). Dispersion curves, mode shapes, stresses and energies of SH and Lamb waves in layered elastic nanoplates with surface/interface effect. *International Journal of Engineering Science, 142*, 170–184.